ISSN 2395-695X (Print)
ISSN 2395-695X (Online)

International Journal of Advanced Research in Biology Engineering Science and Technology (IJARBEST)

Vol. 2, Special Issue 10, March 2016

REVERSIBLE DATA HIDING SCHEME USING PDE BASED INPAINTING PREDICTOR

Asha Jose
Research Scholar, Department Of CSE, Karpagam University
ashajose07@gmail.com

Abstract - Data hacking is very challenging problem in today's internet world. There are number of techniques to secure the data. So, the data hiding in the encrypted image comes into the picture, but occurrence of distortion at the time of data extraction is a main problem. So Reversible Data Hiding (RDH) in encrypted image is used. With this method original cover can be recovered. This paper proposes a novel prediction-based reversible steganography scheme based on image in painting. Reference pixels are chosen adaptively according to the distribution characteristics of the image content.Inpainting technique based on partial differential equations (PDE) is used to generate a prediction image. Finally the histogram of the prediction error is shifted to embed the secret bits reversibly. Because of adaptive strategy for choosing reference pixels and the inpainting predictor, the prediction accuracy is high, and more embeddable pixels are acquired. Thus, the proposed scheme provides a greater embedding rate and better visual quality compared with recently reported methods.

Keywords: Reversible Data Hiding, image inpainting, prediction image, inpainting predictor, PDE.

I. INTRODUCTION

Reversible data hiding, has been studied extensively in recent years, especially for digital images [1]. The property of reversibility means that the original form of the image, before the secret bits were embedded, can be recovered completely after the embedded bits are extracted. Reversible data hiding can be used for medical, military, and legal applications, which do not allow any modification in the digital representation of the cover image due to the risk of misinterpretations.

In general, there are two main categories of reversible data hiding methods for images, i.e., methods based on difference expansion and methods based on histogram shifting [1]–[11]. In 2003, Tian proposed a reversible data hiding method based on difference expansion [1]. In his work, the cover image was divided into a series of no overlapping, neighbouring pixel pairs, and the difference of each pixel pair was doubled. Ni et al. [5] presented a method based on histogram shifting for data hiding. The peak point of the image histogram was selected and the pixel values in the range from its right one to the zero point were increased by one to create one vacant histogram bin for embedding. Recently, many researchers have proposed reversible data hiding methods based on the prediction mechanism [12]–[18]; these methods are extensions of the method based on difference expansion and the method based on histogram shifting. The key idea of the prediction-based method is that the prediction process is conducted first to estimate the cover image pixels, and the prediction error, i.e., the difference between the cover image and the prediction result, is used to embed the secret data by difference expansion or histogram shifting.

ISSN 2395-695X (Print)
ISSN 2395-695X (Online)

International Journal of Advanced Research in Biology Engineering Science and Technology (IJARBEST)

Vol. 2, Special Issue 10, March 2016

II. PROPOSED SCHEME

In our scheme, fewer reference pixels are chosen in the smooth regions of the cover images, while more reference pixels are chosen in the complex regions. This strategy of choosing reference pixels can produce a greater number of possible embeddable pixels and avoid more distortion caused by the embedding procedure. According to the chosen reference pixels, the PDE-based inpainting algorithm can effectively generate the prediction image that has the similar structural and geometric information as the cover image. In order to further achieve higher hiding capacity and less distortion, two groups of peak points and zero points are selected from the histogram of prediction error to embed the secret bits by the shifting operation. The flowchart of the and combined with the prediction result to produce the stego image. The two methods in [13] and [14] utilized neighboring pixels to predict each cover pixel during the scanning of the cover image, and the secret data were embedded by exploiting the expansion of the prediction error.

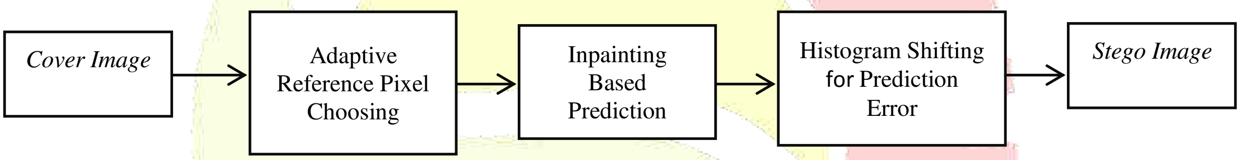

Fig. 1. Flowchart of the embedding procedure.

Hong and Chen [15] tried embedding procedure is shown in Fig. 1. The extraction and recovery procedures are approximately the reverse process of the embedding procedure.

A. Adaptive Reference Pixel Choosing

Denote P(x, y) as the pixel value at the location (x, y) of the cover image P sized M × N. Assume that Q is a binary mask image with the same size as the cover image P, which labels the locations of reference pixels. The pixel P(x, y) is decided as the reference pixel if the corresponding Q(x, y) is equal to 0. The non-reference pixel, which can be used to embed secret information. The initialized mask image Q_0 is satisfied with

$$Q_0(x,y) = \begin{cases} 0, & if\ \ mod\ (x, \mu) = 1\ and\ mod(y, \mu) = 1 \\ 1, & \end{cases} \quad (1)$$

where x = 1, 2, . . . , M; y = 1, 2, . . . , N; and μ denotes the interval between the two neighboring reference pixels. The reference pixels in the smooth region of the cover image lead to a more accurate prediction result than the same number of reference pixels in the complex region [19]. Thus the increase in the number of reference pixels in the complex region to obtain a more accurate prediction result, which may result in greater hiding capacity and better visual quality of the stego image. On the other hand, the number of reference pixels in the smooth region can be reduced moderately to save more possible embeddable pixels, which does not influence the result of the prediction significantly.Based on the above analysis, the reference pixels is adjusted according to the characteristics of the cover image. First, for each pixel P(x, y), where $\mu + 1 \le x \le M - \mu$ and $\mu + 1 \le y \le N - \mu$, $Q_0(x, y)$ can be updated into $Q_1(x, y)$ by

$$Q_1(x,y) = \begin{cases} \Psi(P, x, y, \mu), & \text{if } Q_0(x, y) = 0 \\ 1, & \text{if } Q_0(x, y) = 1 \end{cases} \quad (2)$$

subject to mod(x+y,μ) = 2

ISSN 2395-695X (Print)
ISSN 2395-695X (Online)

International Journal of Advanced Research in Biology Engineering Science and Technology (IJARBEST)

Vol. 2, Special Issue 10, March 2016

where Ψ is a function with a binary output, i.e., 1 or 0, indicating whether the input pixel P(x, y) belongs to the smooth region or not. The detailed representation of the function Ψ is expressed in

$$\Psi(P,x,y,\mu)=\begin{cases} 1, & if\ D \leq T_1 \\ & and\ \ p^{max}_{x,y,\mu} - p^{min}_{x,y,\mu}\ \leq 2\,T_1 + 2 \\ 0\ , & otherwise \end{cases} \tag{3}$$

$$D = \tfrac{1}{3}[P(x-\mu, y) + P(x+\mu, y) + P(x, y-\mu) + P(x, y+\mu) - 4\,p^{min}_{x,y,\mu} \tag{4}$$

(a) (b) (c) (d)

Fig. 2. Binary location masks Q of reference pixels for cover image Lena with different thresholds (μ=4).(a)Binary mask Q with T_1=2, T_2=20.(b)Binary mask Q with T_1=4, T_2=40.(c)Binary mask Q with T_1=6,T_2=60.(d)Binary mask Q with T_1=8,T_2=80

where $P^{max}_{x,y,\mu}$ and $P^{min}_{x,y,\mu}$ are the maximum and the minimum in {P(x−μ, y), P(x+μ, y), P(x, y−μ), P(x, y+μ)}, respectively, and T1 is a predetermined threshold. Second, for each pixel P(x´,y´), where 1 ≤ x´≤ M − μ and 1 ≤ y´≤ N − μ,the $Q_1(x, y)$ of the pixels belonging to the region $x' \leq x \leq x'+\mu$, $y' \leq y \leq y'+\mu$ can be further updated into $Q(x, y)$ by (5) if its corresponding Q_1(x´, y´),Q_1(x´+μ, y´),Q_1(x´,y´+μ), and Q_1(x´+ μ, y´+ μ) are all equal to 0

$$Q(x,y) = \begin{cases} 0, & if\ \Phi(P,x',y',\mu) = 1 \\ Q_{1(x,y)}, & if\ \Phi(P,x',y',\mu) = 0 \end{cases} \tag{5}$$

Subject to x´ ≤ x ≤ x´+μ , y´ ≤ y ≤ y´+μ.

where Φ is also a function with a binary output, i.e., 1 or 0, indicating whether or not the region x′≤x ≤x′+ μ, y ′≤ y ≤ y′+ μ belongs to the complex region. The detailed representation of the function Φ is expressed in

$$\Phi(P,x',y',\mu) = \begin{cases} 1, & \text{if } R > T_1,\ or\ if\ R\ \leq\ T_2 \\ & and\ \ p^{max}_{x',y',\mu} - p^{min}_{x',y',\mu} > 2\,T_2 + 2 \\ 0, & otherwise \end{cases} \tag{6}$$

$$R = \tfrac{1}{3}[P(x',y')+P(x'+\mu,y')+P(x',y'+\mu)+P(x'+\mu, y'+\mu) - 4\,P^{min}_{x',y',\mu}]$$

(7)

where $P^{max}_{x',y',\mu}$ and $P^{min}_{x',y',\mu}$are the maximum and the minimum in {P(x´, y´), P(x´+ μ, y´), P(x´, y´+ μ), P(x´+ μ, y´+ μ)},respectively, and T_2 is a predetermined threshold. After these two steps, the final mask image *Q* can be produced, which indicates the locations of the reference pixels for the cove image *P*. Fig. 2 illustrates the mask images *Q* for cover image *Lena* with different thresholds, i.e., T_1 and T_2, and μ is set to4. The black dots in Fig. 2(a)–(d) correspond to the locations of the reference pixels for *Lena*. It should be noted that the same reference pixels can be exploited on the receiver side, because they are unchanged during the embedding procedure. The selected reference pixels in the cover image are used to generate the prediction image and the detailed prediction process is described in the following section.

B. Pixel Prediction Based on Image Inpainting

After all reference pixels in the cover image have been decided, the non reference pixels are predicted by the image inpainting technique to generate the prediction image. The inpainting-based prediction process is totally dependent on the reference pixels of the cover image. Image inpainting, also known as image retouching, is a kind of technique that can fill in or remove the chosen regions of digital images seamlessly [20]–[22]. Recently, some researchers have applied inpainting techniques in image repairing [23], image compression [24], and deinterlacing [25]. Image inpainting is different from conventional image restoration in which the regions to be restored contain both noise and useful information. In image inpainting, however, the missing or damaged areas generally contain no useful information. Therefore, the task is to generate or create image regions that initially do not exist at all, based on the available information in the close neighbourhood.

Currently, there are several categories of inpainting methods, and the category that is the most widely used is based on PDE. By iteratively solving the numerical representation of a PDE, the inpainting methods manage to propagate the information of gray values smoothly from surrounding areas into region W to be inpainted along a specific direction. The inpainting process is terminated when
the gray values in the computation domain reach a steady state. This paper borrows the idea of treating the problem of pixel prediction from image inpainting, in which the useful information of reference pixels is used to estimate the non reference pixels appropriately. A curvature driven diffusion (CDD)-based inpainting method with a third-order PDE is utilized to implement pixel prediction. This method, in fact, represents an anisotropic diffusion process based on a total variation model [21], and the intensity of diffusion is related to the curvature κ of the pixels for prediction [see (8)–(10)]

$$\frac{\partial P(x,y;t)}{\partial t} = div\left[\frac{\varphi|\mathcal{K}|}{|\nabla P(x,y;t)|}\nabla P(x,y;t)\right]\forall(x,y)\in\Omega \tag{8}$$

$$\mathcal{K} = div\left[\frac{\nabla P}{|\nabla P|}\right] = \frac{P_{xx} - 2P_xP_yP_{xy} + P_{yy}P_x^2}{(P_x^2+P_y^2)^3/_2} \tag{9}$$

$$\varphi(\omega) = \omega^\lambda, \omega > 0\,, \lambda \geq 1 \tag{10}$$

where t is the time index, $\Omega$is the set of all (*x, y*) pairs that satisfy *Q*(*x, y*) = 1, and div(•) is the divergence operator. While solving the PDE in (8) using the finite difference method, the useful information of reference pixels, which are in the surroundings of the non reference

pixels and correspond to $Q(x, y) = 0$, can be propagated into region Ω successfully. The solution P_e of (8) is the final prediction result of the
cover image. Because the CDD-based inpainting model satisfies the connectivity principle of human visual perception, the prediction
image P_e can reflect the structural and geometric information of the original cover image effectively. Therefore, good similarity between the cover image and the prediction image can be achieved. Fig. 3 shows the prediction results based on CDD inpainting according to the corresponding mask images Q of the reference pixels in Fig. 2. Under the same condition of mask images, the prediction results of CDD inpainting have better similarity with the cover image, compared with the results of the classic nearest neighbour interpolation and bilinear interpolation. Table I gives their peak signal-to-noise ratio (PSNR) values of the prediction results for *Lena*. The prediction result of CDD inpainting is compared with the gradient adjusted prediction (GAP) method in [17]. In the GAP method, the two topmost rows and the two leftmost columns are kept unchanged, and each of the residual pixels is predicted progressively in raster-scanning order by the seven neighbouring pixels in its up and left regions. The PSNR value of the GAP prediction result for *Lena* is 32.02 dB. With the reference pixels shown in Fig. 2(b), our CDD inpainting method can achieve 33.62 dB for the prediction result of *Lena*, as shown in Fig. 3(b).

Fig. 3. Prediction results based on CDD inpainting according to the corresponding mask images Q of reference pixels in Fig .2.
(a)PSNR = 37.06 dB. (b) PSNR = 33.62 dB (c) PSNR =31.29 dB (d) PSNR = 29.68 dB

TABLE I

PSNR VALUES OF PREDICTION RESULTS FOR Lena (μ=4)

	PSNR (dB)			
	T1= 2, T2= 20,	T1=4, T2=40	T1=6, T2=60	T1=8 T2=80
Nearest neighbour interpolation	35.78	31.97	29.65	28.08
Bilinear interpolation	36.76	32.93	30.58	28.92
CDD in painting	37.06	33.62	31.29	29.68

the results of the classic nearest neighbor interpolation and bilinear interpolation. Table I gives their peak signal-to-noise ratio (PSNR) values of the prediction results for *Lena*. The

ISSN 2395-695X (Print)
ISSN 2395-695X (Online)

International Journal of Advanced Research in Biology Engineering Science and Technology (IJARBEST)

Vol. 2, Special Issue 10, March 2016

prediction result of CDD inpainting was compared with the gradient adjusted prediction (GAP) method in [17]. In the GAP method, the two topmost rows and the two leftmost columns are kept unchanged, and each of the residual pixels is predicted progressively in raster-scanning order by the seven neighbouring pixels in its up and left regions. The PSNR value
of the GAP prediction result for *Lena* is 32.02 dB. With the reference pixels shown in Fig. 2(b), our CDD inpainting method can achieve 33.62 dB for the prediction result of *Lena*, as shown in Fig. 3(b).

C. Embedding Procedure

During the embedding procedure, the difference image *E*, i.e., the prediction error between *P* and *Pe*, is modified according to the istribution of its histogram and the embedding secret bits. Then, the modified difference image *E´* is added to the prediction image *Pe*to generate the final stego image *Ps*. The detailed steps of the embedding procedure are listed as follows.

Step 1) After the prediction image $P_e$is obtained using the mask image *Q* and the CDD-based inpainting ,the difference image *E* can be easily calculated as

$$E = P - P_e \tag{11}$$

Step 2) Generate the histogram *He* of the difference image *E*. Denote two abscissa values of *He*, corresponding to the highest peak point and the second highest peak point, as $\alpha 1$ and $\alpha 2$, respectively. Thus, there are two cases according to the relationship between $\alpha 1$ and $\alpha 2$

$$\begin{aligned} &\text{Case I} : \text{if } \alpha 1 - \alpha 2 > 0 \\ &\text{Case II} : \text{if } \alpha 1 - \alpha 2 < 0. \end{aligned} \tag{12}$$


(a) (b) (c) (d)

Fig .4.Stego images for Lena with corresponding parameters in Fig. 2. (a) PSNR = 51.04 dB (b) PSNR = 49.96 dB (c) PSNR = 49.40 dB (d) PSNR = 49.22 dB

Step 3) If H_e matches Case I, from $\alpha 1$ to its right, search the first appearing zero point denoted as $\beta 1$ ($\alpha 1 < \beta 1$),
and from $\alpha 2$ to its left, search the first appearing zero point denoted as $\beta 2$ ($\beta 2 < \alpha 2$). Otherwise, search $\beta 1$
from $\alpha 1$ to its left ($\beta 1 < \alpha 1$) and search $\beta 2$ from $\alpha 2$ to its right ($\alpha 2 < \beta 2$).

Step 4) After obtaining $\alpha 1$, $\beta 1$, $\alpha 2$, and $\beta 2$, conduct raster scanning for the pixels *E*(*x*, *y*) that correspond to *Q*(*x*, *y*) = 1 in the difference image. If H_e matches Case I, each scanned *E*(*x*, *y*) is modified to *E* ′(*x*, *y*) using (13) in order to fulfill the embedding procedure.

Otherwise, if H_e matches Case II, *E´*(*x*, *y*) can also be acquired using (14), which changes (13) by substituting$\alpha 1$ for $\alpha 2$, $\alpha 2$ for $\alpha 1$, $\beta 1$ for $\beta 2$, and $\beta 2$ for $\beta 1$. It should be noted that each binary secret bit *S* for hiding is only embedded when the scanned *E*(*x*, *y*) is equal to $\alpha 1$ or $\alpha 2$.

ISSN 2395-695X (Print)
ISSN 2395-695X (Online)

International Journal of Advanced Research in Biology Engineering Science and Technology (IJARBEST)

Vol. 2, Special Issue 10, March 2016

$$E'(x,y) = \begin{cases} E(x,y)+1, & \text{if } E(x,y) = \alpha_1 \text{ and } S = 1 \\ & \text{or if } \alpha_1 < E(x,y) < \beta_1 \\ E(x,y)-1, & \text{if } E(x,y) = \alpha_2 \text{ and } S = 1 \\ & \text{or if } \beta_2 < E(x,y) < \alpha_2 \\ E(x,y), & \text{if } E(x,y) = \alpha_1 \text{ or } \alpha_2 \text{ and } S = 1 \\ & \text{or otherwise} \end{cases} \quad (13)$$

subject to Q(x,y) = 1

$$E'(x,y) = \begin{cases} E(x,y)+1, & \text{if } E(x,y) = \alpha_2 \text{ and } S = 1 \\ & \text{or if } \alpha_2 < E(x,y) < \beta_2 \\ E(x,y)-1, & \text{if } E(x,y) = \alpha_1 \text{and } S = 1 \\ & \text{or if } \beta_1 < E(x,y) < \alpha_1 \\ E(x,y), & \text{if } E(x,y) = \alpha_1 \text{ or } \alpha_2 \text{ and } S = 1 \\ & \text{or otherwise} \end{cases} \quad (14)$$

subject to Q(x,y) = 1

Step 5) Add the modified E´to the prediction image P_e to produce the final stego image *Ps* [see (15)]

$$Ps = Pe + E'. \quad (15)$$

It should be noted that if $\beta 1$ or $\beta 2$ do not exist in *He* mentioned in Step 3, zero points should be created. For example, in Case I, if zero point $\beta 1$ does not exist, the locations of the cover pixels corresponding to the lowest bin of H_e on the right side of $\alpha 1$ are recorded by a binary matrix Γ_z, and then the lowest bin is modified to zero and its abscissa value is used as the zero point $\beta 1$. In the extraction and recovery procedures, the binary matrix $\Gamma_z$can be utilized to localize and restore the cover pixels corresponding to the original lowest bin of *He* on the right side of $\alpha 1$. Additionally, in order to avoid underflow and overflow problems, the locations of the cover pixels was recorded, whose values equal 0 or 255and their corresponding prediction errors are in the ranges of two groups of peak points and zero points in *He*, and then modify their values to 1 and 254, respectively. The recorded information is stored in a binary matrix Γ_f, which can assist in recovering these pixels to their original values, i.e., 0 and 255 in the extraction and recovery procedures. Usually, the two binary matrices, i.e., Γ_z and Γ_f, that served as the location map are sparse, and they can be compressed easily using a run-length coder. The compressed

ISSN 2395-695X (Print)
ISSN 2395-695X (Online)

International Journal of Advanced Research in Biology Engineering Science and Technology (IJARBEST)

Vol. 2, Special Issue 10, March 2016

results of Γ_z and Γ_f are concatenated into a binary sequence Γ. After the above steps have been implemented, the embedding procedure is finished and the stego image *Ps* is obtained. The total number of embedded secret bits, i.e., total hiding capacity, is equal to the number of the difference image pixels that satisfy $E(x, y) = \alpha 1$ or $\alpha 2$ and $Q(x, y) = 1$. In fact, the embedding procedure is equivalent to shifting the histogram of the difference image between the two groups of peak point and zero point, i.e., $\alpha 1$, $\beta 1$ and $\alpha 2$, $\beta 2$, by one level at most [see (13)
and (14)]. Consequently, only the corresponding cover image pixels $P(x, y)$ are increased or decreased by one gray level at most to form the stego image *Ps*. Therefore, the visual quality of the stego image is satisfactory. Fig. 4 illustrates the stego images for *Lena* with the corresponding parameters mentioned in Fig. 2.

D. Extraction and Recovery Procedures

During the extraction procedure, the embedded bits can be extracted, and the cover image can be recovered losslessly. To guarantee the success of extraction and recovery, the parameters, μ, $T1$, $T2$, $\alpha 1$, $\beta 1$, $\alpha 2$, $\beta 2$, Γ, must be transmitted to the receiver side through the secure channel. Suppose that the size of the stego image *Ps* is not changed during transmission. Because the same strategy for choosing reference pixels is utilized and since the reference pixels are intact during the embedding procedure, the same prediction image *Pe* can be acquired from the stego image *Ps* by applying CDD-based inpainting. The detailed steps of the extraction and recovery procedures are listed as follows.

Step 1) After the same prediction image *Pe* is obtained from the stego image *Ps* by the same method used in the embedding procedure, the difference between *Ps* and *Pe*, i.e., E', can be acquired easily.

Step 2) According to the received $\alpha 1$ and $\alpha 2$, the case to which the embedding procedure belongs can be determined by (12).

Step 3) Conduct raster-scanning for the pixels $E'(x, y)$ that correspond to the locations of the non reference pixels for the stego image *Ps*.

If the embedding procedure belongs to Case I, (16) can be utilized to extract each embedded secret bit *S* and to modify each scanned $E'(x, y)$ into $E'_c(x, y)$. Otherwise, (17) is utilized instead. It should be noted that each hidden binary bit S is extracted only when the scanned $E'(x, y)$ is equal to $\alpha 1$, $\alpha 2$, $\alpha 1 + 1$, or $\alpha 2 + 1$

Figure.5. Six standard test images (a) Lena (b) Lake (c) Barbara (d) Goldhill(e) Tiffany (f)Peppers

ISSN 2395-695X (Print)
ISSN 2395-695X (Online)

International Journal of Advanced Research in Biology Engineering Science and Technology (IJARBEST)

Vol. 2, Special Issue 10, March 2016

$$E'_c(x,y) = \begin{cases} E'(x,y)+1, \textit{and } S=1, & \textit{if } E'(x,y) = \alpha_2 - 1 \\ E'(x,y)-1, \text{and S} = 1, & \text{if } E'(x,y) = \alpha_1 + 1 \\ E'(x,y), \text{and S} = 0, & \text{if } E'(x,y) = \alpha_1 \textit{ or } \alpha_2 \\ E'(x,y)+1, & \text{if } \beta_2 \le E'(x,y) < \alpha_2 \\ E'(x,y)-1, & \text{if } \alpha_1 < E'(x,y) \le \beta_1 \\ E'(x,y), & \textit{otherwise} \end{cases} \quad (16)$$

$$E'_c(x,y) = \begin{cases} E'(x,y)+1, \textit{and } S=1, & \textit{if } E'(x,y) = \alpha_1 - 1 \\ E'(x,y)-1, \text{and S} = 1, & \text{if } E'(x,y) = \alpha_2 + 1 \\ E'(x,y), \text{and S} = 0, & \text{if } E'(x,y) = \alpha_1 \textit{ or } \alpha_2 \\ E'(x,y)+1, & \text{if } \beta_1 \le E'(x,y) < \alpha_1 \\ E'(x,y)-1, & \text{if } \alpha_2 < E'(x,y) \le \beta_2 \\ E'(x,y), & \textit{otherwise} \end{cases} \quad (17)$$

Step 4) Add E'_c to the prediction image P_e to produce the recovered image P_c [see (18)].$E(x,y)E'(x,y)\ \alpha_2\beta_1\alpha_1\beta_2$

$$Pc = Pe + E'_c \quad (18)$$

After the above steps have been implemented, all embedded secret bits S are extracted correctly, and the recovered image Pc is obtained. Actually, the extraction procedure is equivalent to shifting the histogram H'_e of E´ back to the histogram H_e of E [see (13), (14), (16), and (17)] and $E'_c$is exactly equal to E. Thus, it can be found from (11) and (18) that the recovered image P_c is completely the same as the original cover image *P*.

III. CONCLUSION

In order to enhance the availability of embeddable space and reduce the prediction error simultaneously, an adaptive strategy based on the distribution characteristics of image content was adopted, in which fewer reference pixels were chosen in the smooth regions of cover images and more referencepixels were chosen in the complex regions. According to the reference pixels that were chosen, the PDE-based inpainting algorithm using the CDD model can generate the prediction image effectively that has the similar structural and geometric information as the cover image. Through the use of the adaptive strategy for choosing reference pixels and the inpainting predictor, the accuracy of the prediction result was high, and larger numbers of embeddable pixels are acquired. To further reduce the distortion caused by embedding, two groups of peak points and zero points are selected from the histogram of the prediction error to embed the secret bits reversibly by the shifting operation. Because the same reference pixels can be exploited, the prediction result of the extraction procedure is
the same as that of the embedding procedure. Thus, the embedded secret data can be extracted from the stego image correctly, and the original cover image can be recovered losslessly. Compared with other schemes that have been reported recently, the proposed scheme has better performances with respect to the embedding rate and the visual quality of the stego image. In the current stage, parameters, such as the thresholds for the reference

pixel choosing, are predetermined by experience or chosen by using trial and error. In our future studies, the
stochastic optimization algorithms, such as the particle swarm optimization, can be utilized to optimize these parameters to achieve the near optimal performances of the proposed scheme. Further improvements will also include using the faster numerical method to solve the high order PDE of theinpainting model so that the pixel prediction can be implemented more efficiently.

REFERENCES

[1] J. Tian, "Reversible data embedding using a difference expansion," IEEE Trans. Circuits Syst. Video Technol., vol. 13, no. 8, pp. 890–896, Aug. 2003.
[2] M. U. Celik, G. Sharma, A. M. Tekalp, and E. Saber, "Lossless generalized-LSB data embedding," IEEE Trans. Image Process., vol. 14, no. 2, pp. 253–265, Feb. 2005.
[3] C. C. Chang and C. Y. Len, "Reversible steganographic method using SMVQ approach based on declustering," Informat. Sci., vol. 177, no. 8, pp. 1796–1805, 2007.
[4] C. C. Chang, C. C. Lin, C. S. Tseng, and W. L. Tai, "Reversible hiding in DCT-based compressed images," Informat. Sci., vol. 177, no. 13, pp. 2768–2786, 2007.
[5] Z. C. Ni, Y. Q. Shi, N. Ansari, and W. Su, "Reversible data hiding," IEEE Trans. Circuits Syst. Video Technol., vol. 16, no. 3, pp. 354–362, May 2006.
[6] A. M. Alattar, "Reversible watermark using the difference expansion of a generalized integer transform," IEEE Trans. Image Process., vol. 13, no. 8, pp. 1147–1156, Aug. 2004.
[7] C. C. Chang and T. C. Lu, "A difference expansion oriented data hiding scheme for restoring the original host images," J. Syst. Software, vol. 79, no. 12, pp. 1754–1766, 2006.
[8] W. L. Tai, C. M. Yeh, and C. C. Chang, "Reversible data hiding based on histogram modification of pixel differences," IEEE Trans. Circuits Syst. Video Technol., vol. 19, no. 6, pp. 906–910, Jun. 2009.
[9] M. Fallahpour, D. Megias, and M. Ghanbari, "Reversible and highcapacity data hiding in medical images," IET Image Process., vol. 5, no. 2, pp. 190–197, 2011.
[10] C. Y. Yang, C. H. Lin, and W. C. Hu, "Reversible data hiding by adaptive IWT-coefficient adjustment," J. Informat. Hiding Multimedia Signal Process., vol. 2, no. 1, pp. 24–32, 2011.
[11] H. C. Huang and W. C. Fang, "Authenticity preservation with histogrambased reversible data hiding and quadtree concepts," Sensors, vol. 11, no. 10, pp. 9717–9731, 2011.
[12] D. M. Thodi and J. J. Rodriguez, "Expansion embedding techniques for reversible watermarking," IEEE Trans. Image Process., vol. 16, no. 3, pp. 721–730, Mar. 2007.
[13] H. W. Tseng and C. P. Hsieh, "Prediction-based reversible data hiding," Informat. Sci., vol. 179, no. 14, pp. 2460–2469, 2009.
[14] C. F. Lee, H. L. Chen, and H. K. Tso, "Embedding capacity raising in reversible data hiding based on prediction of difference expansion," J. Syst. Software, vol. 83, no. 10, pp. 1864–1872, 2010.
[15] W. Hong and T. S. Chen, "Reversible data embedding for high quality images using interpolation and reference pixel distribution mechanism," J. Visual Commun. Image Representation, vol. 22, no. 2, pp. 131–140, 2011.
[16] Z. Zhao, H. Luo, Z. M. Lu, and J. S. Pan, "Reversible data hiding based on multilevel histogram modification and sequential recovery," Int. J. Electron. Commun., vol. 65, no. 10, pp. 814–826, 2011. [17] M. Fallahpour, "Reversible image data hiding based on gradient adjusted prediction," IEICE Electron. Express, vol. 5, no. 20, pp. 870–876, 2008.

ISSN 2395-695X (Print)
ISSN 2395-695X (Online)

International Journal of Advanced Research in Biology Engineering Science and Technology (IJARBEST)

Vol. 2, Special Issue 10, March 2016

[18] L. X. Luo, Z. Y. Chen, M. Chen, X. Zeng, and Z. Xiong, "Reversible image watermarking using interpolation technique," IEEE Trans. Informat. Forensics Security, vol. 5, no. 1, pp. 187–193, Mar. 2010.
[19] X. Wang, "Laplacian operator-based edge detectors," IEEE Trans. Pattern Analysis Mach. Intelligence, vol. 29, no. 5, pp. 886–890, May 2007. [20] M. Bertalmio, G. Sapiro, V. Caselles, and C. Ballester, "Image inpainting," in Proc. 27th Int. Conf. Comput. Graphics Interactive Techniques, Jul. 2000, pp. 417–424.
[21] T. F. Chan and J. Shen, "Nontexture inpainting by curvature-driven diffusions," J. Visual Commun. Image Representation, vol. 12, no. 4, pp. 436–449, 2001.
[22] C. Qin, F. Cao, and X. Zhang, "Efficient image inpainting using adaptive edge-preserving propagation," Imag. Sci. J., vol. 59, no. 4, pp. 211–218, 2011. [23] C. Qin, S. Wang, and X. Zhang, "Simultaneous inpainting for image structure and texture using anisotropic heat transfer model," Multimedia Tools Appl., vol. 56, no. 3, pp. 469–483, 2012.
[24] D. Liu, X. Y. Sun, F. Wu, S. P. Li, and Y. Q. Zhang, "Image compression with edge-based inpainting," IEEE Trans. Circuits Syst. Video Technol., vol. 17, no. 10, pp. 1273–1287, Oct. 2007.
[25] C. Ballester, M. Bertalmío, V. Caselles, L. Garrido, A. Marques, and F. Ranchin, "An inpainting-based deinterlacing method," IEEE Trans. Image Process., vol. 16, no. 10, pp. 2476–2491, Oct. 2007.